

SPECTROMETRIC AND PHOTOGRAPHIC ANALYSIS OF A  
LASER-PRODUCED HYDROGEN PLASMA

Kurt Dieter Wachsmuth



# NAVAL POSTGRADUATE SCHOOL

## Monterey, California



# THESIS

SPECTROMETRIC AND PHOTOGRAPHIC ANALYSIS  
OF  
A LASER-PRODUCED HYDROGEN PLASMA

by

Kurt Dieter Wachsmuth

Thesis Advisor:

F. Schwirzke

June 1973

T154798

*Approved for public release; distribution unlimited.*



Spectrometric and Photographic Analysis  
of  
a Laser-Produced Hydrogen Plasma

by

Kurt Dieter Wachsmuth  
Lieutenant Commander, Federal German Navy

Submitted in partial fulfillment of the  
requirements for the degree of

MASTER OF SCIENCE IN PHYSICS

from the  
NAVAL POSTGRADUATE SCHOOL

1972



## ABSTRACT

Light from a neodymium glass laser was focused in hydrogen gas at pressures from 20 mTorr to 9.16 atm in order to produce optical breakdown. The forward scattered light from the breakdown region was spectrally analyzed with a grating spectrograph from 10,300 to 10,900 Å. It was found that the spectral distributions exhibited no distinguishable frequency shift. However, the absorption of the laser light depended on frequency and gas pressure. The time dependence of the onset of absorption was determined by comparing the cell beam with a beam-split reference beam that bypassed the pressure cell. The light scattered at an angle of  $90^\circ$  was photographed with a high speed image converter camera in the framing mode. This revealed evidence of self-focusing during the time the laser light was on. The plasma parameters were calculated from the kinetic theory of ideal gases and the theory of ionized gases, assuming complete ionization. The results of this study were compared to results published in the current literature. Agreement was good, especially in the case of self-focusing.





## TABLE OF CONTENTS

I.	INTRODUCTION-----	4
II.	THEORY -----	7
III.	EXPERIMENTAL PROCEDURE -----	18
IV.	DATA -----	23
V.	RECOMMENDATION-----	33
	ILLUSTRATIONS -----	35
	LIST OF REFERENCES -----	46
	INITIAL DISTRIBUTION LIST -----	48
	FORM DD 1473 -----	49



## I. INTRODUCTION

The creation of a hot dense plasma by means of a giant pulse laser is of prime interest to the field of plasma physics. Nuclear fusion occurs and nuclear energy is released if a deuterium plasma is heated to a sufficiently high temperature. Laser heating of the plasma can eventually produce the high temperatures needed in this process. The conductivity of a plasma increases with temperature, and if the plasma density is high enough a large fraction of the energy in the laser beam may be reflected. However, the resistivity of the plasma may increase greatly by an instability in the plasma. A laser pulse of sufficient intensity may cause instability in the plasma leading to enhanced absorption, and heat the plasma turbulently to higher temperatures than could be attained by the classical absorption process of electron-ion collisions.

A hot dense plasma can be produced by focusing a pulse from a Q-switched laser onto a solid target. The density and temperature gradients in this plasma cover the entire range of conditions from an underdense to an overdense plasma. It is obviously difficult to investigate the processes of absorption and scattering in a controlled fashion in this system. This problem can be overcome, however, by using laser breakdown of a hydrogen gas in a pressure cell to produce the



plasma. Thus the plasma density can be controlled by the background pressure selected.

The purpose of this study was to measure the absorption and the spectral distribution of the forward scattered light of the laser produced hydrogen plasma under pressures from 20 millitorrs to ten atmospheres. It was intended originally to find satellite structures outside the main spectral band of the laser light. These secondary maxima which have been reported for the case of solid deuterium targets as a consequence of the soliton theory by M. Decroisette et alii [Ref. 1] could not be found, even though the search for these expected phenomena was extended over a range of 300 Å<sup>o</sup>ngströms about the central laser line. It was therefore decided to examine more closely the absorption characteristics of the plasma at different wavelengths in the laser spectrum. This was augmented by the study of the breakdown and generation of the plasma by means of high speed photography. The image converter camera used for this purpose revealed the structure of the plasma during the time the laser pulse was on. This led to the discovery of a self-focusing effect in the plasma which may increase the absorption rate above the classical limits by nonlinear effects.

A giant pulse neodymium laser was used to create a hydrogen plasme inside a pressure cell. The forward scattered light was analyzed by a grating spectrograph equipped with a properly biased



semiconductor photodiode. In order to avoid damage to the image converter high-speed camera only the light scattered at an angle of 90 degrees was used for photographic analysis.

The upper limits of the plasma parameters, density and temperature, were estimated by using the kinetic theory of ideal gases and the basic theory of ionized gases slightly modified for the pertinent conditions of this study. This gave values for the plasma density and temperature which were comparable to data published in the current literature. Emphasis in this study was put on the pressure range for which laser induced gas breakdown occurred. Thus both high speed photography and spectral analysis were used to analyze the laser created plasma over a wide pressure range.





## II. THEORY

The density of the hydrogen gas used in this study can be derived from the laws of the kinetic theory of an ideal gas. The fundamental equation is the ideal gas law given by

$$(1) \quad p V = \eta R T$$

where  $p$  means the pressure of the gas, measured in  $\text{N/m}^2$ ,  $V$  the volume measured in  $\text{m}^3$ ,  $\eta$  the number of moles in a bounded volume,  $R$  the ideal gas constant, and  $T$  the temperature in degrees Kelvin.

Using

$$(2) \quad \eta R / V = n k$$

where  $n$  is the number density in  $\text{m}^{-3}$ , and  $k$  is the Boltzmann constant, this equation can be rewritten as

$$(3) \quad p = n k T.$$

At room temperature ( $288^{\circ}$  Kelvin) there are thus

$$(4) \quad n = 2.52 \times 10^{20} p$$

molecules in the hydrogen gas. Since each molecule contains two protons and two electrons the fully ionized plasma would contain  $2 n$  electrons and  $2 n$  protons. Assuming a pressure of three atmospheres which is equivalent to  $3.04 \times 10^5 \text{ N / m}^2$  there are  $1.53 \times 10^{26}$  electrons in one cubic meter.

The interaction between the laser light and the hydrogen gas takes place in the focal volume. This focal volume is calculated



from the focal spot diameter and the interaction length. The focal spot diameter is given by [Ref. 2]

$$(5) \quad d = f \theta$$

where  $f$  is the focal length of the lens used and  $\theta$  is the laser beam divergence. Substituting the published beam divergence of  $1.7 \times 10^{-3}$  radians and the measured focal length of 0.053 m,  $d$  is obtained as  $9.01 \times 10^{-5}$  m. The interaction length can be estimated by using the formula for the depth of focus which is the axial distance over which the focal spot diameter is very nearly constant. From Ref. 3 this length is

$$(6) \quad l = 4 \lambda \left( f / \Delta \right)^2$$

where  $\lambda$  is the wavelength of the laser,  $f$  is the focal length of the lens and  $\Delta$  is the entrance spectral diameter of the optical system. Setting  $\Delta$  equal to the laser beam diameter of 0.75 inches the "focal spot length" is  $3.26 \times 10^{-5}$  m. This value, however, is very small compared to the length of the plasma column photographed and measured in the experiment to be about  $3 \times 10^{-3}$  m. Thus the interaction length was assumed to be about a hundred times larger, closer to  $3 \times 10^{-3}$  m. This implies a laser heated volume of  $1.91 \times 10^{-11} \text{ m}^3$ . This agrees with data published in the current literature [Ref. 4].

This initial plasma volume contains  $2.92 \times 10^{15}$  electrons and  $2.92 \times 10^{15}$  protons at a pressure of three atmospheres. Assuming



absorption of a typical laser pulse of six joules this results in an energy density of  $3.14 \times 10^{11} \text{ J / m}^3$ . Every electron or proton could thus receive  $1.03 \times 10^{-15}$  joules which is equivalent to  $6.41 \times 10^3 \text{ eV}$ . This estimated value, however, may be one or two orders of magnitude too high, since the plasma starts to expand and heats the background gas while the laser pulse is still on.

The current literature reports values from ten to 100 eV for a plasma produced by laser breakdown of a gas. N. Ahmad and M. H. Key [Ref. 5] used the soft X-ray flux from the laser plasma, created by absorption of the laser radiation by metal foils of different thickness. They observed a systematic relationship between laser power and plasma temperature. For air at one atmosphere pressure they found plasma temperatures of 40 to 50 eV when they used a ruby laser of 200 megawatts power. P. de Montgolfier [Ref. 6] calculated an equilibrium temperature for helium at a pressure of 1700 torrs of 10 eV when the laser power is 830 megawatts. However, these values have to be interpreted carefully for the purpose of this study. For hydrogen R. I. Soloukhin and Yu. A. Yacobi [Ref. 7] have calculated hydrogen absorption coefficients in dependence on plasma density and temperatures up to about 15 eV.

It seems therefore reasonable for the purpose of this study to assume an electron temperature of 100 electronvolt. It should be noted, however, that reflection of the incident laser light cannot be



of great importance in this process, because in the range of  $\omega > \omega_{pe}$  there is not much reflection to be expected. Thus scattering and collisional transfer of energy to the background gas are believed to be the cause of the discrepancy between the available energy and the estimated electron temperature.

Another important parameter is the power density at the focus of the lens. It is given by [Ref. 2]

$$(7) \quad F = P / A$$

where  $P$  is the laser power and  $A$  is the crosssectional area of the focal spot. Using the typical laser pulse of six joules with a halfwidth time of 25 nanoseconds and  $A = 6.38 \times 10^{-9} \text{ m}^2$  the power density is calculated to be  $3.76 \times 10^{16}$  watts per square meter. This value is sufficient to produce breakdown in the focal volume as can be seen from the high electric field intensity that is associated with it.

The energy density in an electromagnetic wave is given by  $E^2 / 8 \pi$ . If this energy density travels through space an energy density flux is created. In the case of an electromagnetic wave this velocity is the velocity of light,  $c$ . Since the refractive index, which is determined by the ratio of the speeds of light in vacuum and in matter, for hydrogen gas is very close to unity the energy density flux is given by  $E^2 c / 8 \pi$ . This energy density flux can be equated to the power density at the focal crosssectional area. This







yields an electric field intensity of

$$(8) \quad E = \sqrt{8 \pi F / c} .$$

From the proper cgs units  $E$  is evaluated to be  $5.32 \times 10^7$  volts per centimeter for the typical laser pulse of six joules. This value is in agreement with data published in the current literature [Ref. 2].

This high electric field of the laser beam interacts with the free electrons in the hydrogen gas forcing them to oscillate and exchange energy with other electrons and protons by the inverse Bremsstrahlung mechanism.

The absorption of the laser light can be described by Lambert's law. Energy is absorbed over a distance  $L$  by a plasma according to the equation

$$(9) \quad W = W_o ( 1 - e^{-KL} )$$

where  $W_o$  is the laser energy,  $K$  is the absorption coefficient and  $L$  is the interaction length. The classical coefficient for absorption due to electron-ion collisions is [Ref. 8]

$$(10) \quad K = 8\pi Z n_e n_i e^6 \ln\Lambda(\nu) / 3c \nu^2 (2 m_e kT)^{3/2} (1 - \nu_p^2 / \nu^2)^{1/2} .$$

When the plasma frequency is close to the laser frequency the classical absorption length  $L = 1 / K$  is according to Kaw et alii [Ref. 9]

$$(11) \quad L = 5 \times 10^{18} T^{3/2} / n_e \text{ micrometer}$$

where  $T$  is measured in electronvolt and  $n_e$  in  $\text{cm}^{-3}$ . Assuming an electron temperature of 100 eV and an electron density of  $1.53 \times 10^{20} \text{ cm}^{-3}$  the absorption length is  $32.7 \mu\text{m}$ . This is the



same length that was obtained earlier for the focal spot length from equation (6). From camera measurements, however, a total length of the plasma column a hundred times larger was found.

When  $\nu_L$  is larger than  $\nu_p$  the absorption coefficient for the neodymium laser is given by [Ref. 10]

$$(12) \quad K = 1.5 \times 10^{-41} n_e^2 / T^{3/2}$$

if  $n_e$  is measured in  $\text{cm}^{-3}$  and  $T$  in  $\text{keV}$ . For a pressure of three atmospheres and an electron temperature of 100 eV  $K$  is calculated to be  $11.1 \text{ cm}^{-1}$ . If the interaction length is assumed to be 0.3 cm from camera measurements the exponent in equation (9) becomes 3.33 and thus 96.4% of the energy is absorbed in the plasma. This value is consistent with the observed results in this study and in a previous work done by Jim Carlisle [Ref. 11]. However, a change by a factor of ten in the electron temperature to a value of 1 keV produces a large variation in the amount of energy absorbed. In this case only 10% of the energy would be absorbed. If an electron temperature of only 10 eV is assumed  $KL$  is calculated to be 105.3 and an absorption of about 100% is achieved. These calculations indicate the basic necessity for a detailed knowledge of the actual electron density and electron temperature. If these quantities were known the absorption length could be checked by the observed percentage of absorption.



A comparison of these calculated values with figure 3 shows that at three atmospheres the measured absorption is 70% for the central laser line and higher at the sides, 93% for  $10,658 \text{ \AA}^{\circ}$  and 83% for  $10,616 \text{ \AA}^{\circ}$ . The same result was observed at several pressures. This indicates that the sample calculation of the absorption rate carried out above is only an estimate of the actual conditions. It can be said, however, that the electron temperature seems to be in the vicinity of 100 eV. An explanation of the different values of absorption at these different frequencies has still to be found.

As indicated before, a possible explanation could lie in the presence of instabilities in the plasma. This could cause a greater resistivity of the plasma and thus an enhancement of absorption due to moderate ion density fluctuations. In a paper by I. J. Spalding [Ref. 12] several mechanisms are mentioned that can indeed increase the resistivity of the plasma. For the region of interest in this study, however, only a parametric instability discussed by Dubois and Goldman [Ref. 13] is of importance.

If the plasma frequency given by

$$(13) \quad \omega_p^2 = n_e e^2 / m_e \epsilon_0$$

where  $e$  is the electronic charge,  $m_e$  the electron mass, and  $\epsilon_0$  the permittivity of free space, is close to the laser frequency a threshold power density for onset of parametric instability of

$$(14) \quad P_{DG} \geq 10^{-10} n_e T$$





is necessary. For the estimated values of  $n_e$  and  $T$  ( $1.53 \times 10^{20} \text{ cm}^{-3}$  and  $100 \text{ eV}$ )  $P_{DG}$  is calculated to be  $1.53 \times 10^{12} \text{ W / cm}^2$ .

This power density can indeed be reached with the typical six joules pulse.

Self-focusing effects in a hot dense plasma increase the power density immensely. These self-focusing phenomena have been observed by a multitude of authors. A. J. Alcock [Ref. 14] discusses the possible mechanisms and the experimental evidence obtained so far. He found that in hydrogen and other gases a beadlike breakdown structure was obtained when the laser power was slightly above threshold power for breakdown. A summary of Alcock's findings is given below.

He found that fork-like scattering regions could be observed as the laser intensity was increased. The transverse dimension of the scattering region for the laser light was found to be at least an order of magnitude smaller than the focal spot diameter of 50 micrometer. The forward scattered light from an air spark at atmospheric pressure emerged into a well defined cone having an included angle of about thirty degrees. It could also be shown that the forward scattered light was produced at the instant of breakdown, i. e. the time at which the transmission of the nonscattered light decreased sharply. The polarization of the forward scattered light was the same as that of the incident laser light and it was coherent. High resolution Schlieren photographs revealed filamentary regions with a high index of refraction.





These filaments had a diameter less than ten micrometer and were running between blobs of plasma separated by several hundred micrometers. By interferometric techniques these filaments could be shown as extremely narrow channels of high density plasma.

Although many of the described experimental results indicate the presence of self-focusing effects, little is known about the actual physical process involved. Since all of the experimental evidence obtained so far applies to laser induced breakdown, self-focusing could occur during one or more stages of spark formation:

- a) immediately prior to breakdown in the neutral gas
- b) during the cascade ionization process
- c) after a high density plasma has been formed.

During each of these stages it is possible to identify non-linear processes capable of producing refractive index changes of the appropriate sign. Thus in case a) either electrostriction or the electrooptical Kerr effect could provide the required nonlinearity. If the threshold powers are of the order of tens of megawatts electrostriction is most important and if they are in the gigawatt range the Kerr effect is dominant. For relatively low power levels electrostriction has been observed to cause self-focusing in a transparent medium. Kerr indicates in his paper [Ref. 15] that a computer simulation of the self-focusing effect in glass shows an extremely rapid upstream motion of the focal points while the diameter of the beam collapses to a relatively constant radius.



The electrostrictive force in a homogeneous medium tends to draw the material into the region of a high electric field. The electric field in turn induces dipoles in the medium which will experience a force proportional to the gradient of the square of the electric field, that is to the gradient of the intensity. The greatest magnitude of force is found at half-width, i. e. at the edge of the beam. This causes a maximal compression on the axis. Thus a laser pulse of threshold power for electrostriction can create its own waveguide. Pulses of higher power show self-focusing. The strong electric field of the laser beam exerts an electrostrictive force on the material through which the beam passes. The force drives a sound wave. As this sound wave develops it alters the index of refraction. This in turn changes the trajectory of the beam and modifies the electrostrictive force.

In the model for self-focusing during cascade ionization processes the neutral gas is replaced by a mixture of electrons, ions, and neutral atoms in different stages of excitation after the cascade ionization process has begun. Since the absolute polarizability of excited atoms exceeds that of unexcited or ionized atoms the defocusing effect of the free electrons due to a reduction of refractive index with higher electron density at the center might be cancelled and a net self-focusing effect results. But in this case there is not enough experimental evidence obtained so far to confirm this model. Also the hydrogen



plasma will probably be fully ionized within a short time after onset of breakdown.

Then the possibility of self-focusing in the resulting plasma (stage c) must be considered. The existence of numerous nonlinear plasma effects is well known. The lateral decrease of the laser beam intensity causes a ponderomotive force  $f_p$  which can be separated into two terms. The linear term is the thermokinetic force  $f_{th}$  and the nonlinear term is the nonlinear force  $f_{NL}$  due to the quadratic terms of the electromagnetic field components. H. Hora has shown in his paper [Ref. 16] that this nonlinear force can be written as

$$(15) \quad f_{NL} = \frac{E^2 \omega_p^2}{16 \pi \omega^2 n_r^2} \cdot \partial n_r / \partial r$$

where  $n_r$  is the complex index of refraction. When absorption of the laser light by the plasma takes place,  $f_{NL}$  exceeds the thermokinetic force and a rarefaction of the plasma about the beam axis occurs.

Since the index of refraction of a plasma is given by [Ref. 17]

$$(16) \quad n_r = 1 - 4.5 \times 10^{14} \lambda^2 n_e$$

where  $\lambda$  is the wavelength of the laser in cm and  $n_e$  is the electron density in  $\text{cm}^{-3}$ ,  $n_r$  increases with  $n_e$  decreasing.

Thus the rarefaction of the plasma provides the right increase of the index of refraction to allow total internal reflection of the laser beam and self-focusing occurs.



### III. EXPERIMENTAL PROCEDURE

A Korad Model K-1500 neodymium laser system was used throughout the study. This system has the following characteristics:

Energy	3 to 9 Joules
Pulse width	22 to 28 nanoseconds
Peak power	200 to 350 Megawatts
Wavelength	1.06 micrometers
Beam diameter	0.75 inch

A pressure cell which had been constructed by Jim Carlisle in a previous work was used to contain hydrogen gas at pressures from 20 millitorrs to ten atmospheres. This cell had a center cavity volume of approximately 12 inch<sup>3</sup>. It was outfitted with two inch diameter entrance and exit windows and two by three inch side windows. All windows were of Pyrex 7913 tempered glass which has a 91% transmission at the laser wavelength. The top opening was used for the gas supply plumbing and the bottom was closed by a brass plate containing tungsten wires which were used to focus the high speed camera looking through the side window. A forepump was used to evacuate the whole system and to lower the gas pressure below one atmosphere. Nitrogen gas was used before and after each experimental run to purge the whole system in order to insure a safe operation.







The laser beam was focused at the center of the cell with a 5.3 cm focal length doubly convex lens  $L_2$  mounted behind the entrance window of the cell. The same type of lens  $L_1$  was used in a similar fashion at the exit window to focus the diverging forward scattered light to the entrance slit of a grating spectrometer constructed in 1968 by George Orlicki. This grating spectrometer had a grating constant of  $8340 \text{ \AA}$  and allowed the measurement of wavelengths up to  $16,471.5 \text{ \AA}$  in first order diffraction. In order to get a reference pulse for each laser shot a 4% beamsplitter  $B_3$  was mounted ahead of the cell so that a system of two plane mirrors in the optical plane of the system, ten meters apart, could provide a delay of 87 nanoseconds (Fig. 1). The last reflection off mirror 2 was focused on the entrance slit of the spectrometer by a cylindrical lens  $L_3$  of 1 meter focal length. Due to the alignment of the cell and the spectrometer the exit beam from the cell and the reference beam from the mirror system had to be reflected by beamsplitters  $B_2$  and  $B_4$  at an angle of about 45 degrees to the light path to insure normal incidence on the entrance slit of the spectrometer.

The spectrometer had entrance and exit slits of 300 micrometers width which allowed a spectral discrimination of  $0.1 \text{ \AA}$  in the visible region. The grating inside the spectrometer was moveable by a lever arm sliding along a screwed thread to allow for the selection of the wavelength region of interest. The screwed threat was attached to a



digital counter which simplified the setting of the desired wavelength. The calibration of the spectrometer was obtained by observing the prominent lines of a mercury arc lamp which in second order diffraction encompasses the spectral region of interest in this study, 10,300 to 10,900 Å. Multiple checks at different orders of diffraction showed that the digital counter reading was directly proportional to the wavelength selected. Thus a daily check of the mercury green spectral line in second order diffraction was considered to be sufficient for the compensation of the play in the mechanical parts. The intensity of the cell beam and the reference beam were displayed on a Tektronix 7904 using a UDT PIN 10 photodiode as a detector. This photodiode was biased to provide a rise time of five nanoseconds which seemed to be sufficient for the monitoring of the intensities of both beams at the predialed wavelength setting.

The energy in each laser pulse was determined by a laser pulse monitor which consisted of a 4% beamsplitter  $B_1$  that sent a sample of the laser pulse via a magnesium oxide diffuser block to the Korad K-D1 detector. This detector had an internal integrating circuit whose output was displayed on a Tektronix 564B storage scope. The calibration of this arrangement was carried out by Leslie McKee in a previous work, and his calibration chart was utilized throughout the study. The same K-D1 photodiode was also used to trigger the Tektronix oscilloscope and to obtain the laser pulse profile every morning to check for the performance of the neodymium glass laser.



The high speed image converter camera IMACON 600 was used to obtain sequential pictures of the developing plasma in the focal region of the cell. It was equipped with an Eastman-Kodak Aero-Ektar f:2.5 optical system of 178 mm focal length which allowed an approximate magnification of 1:2. The camera was focused on the nine vertically erect tungsten wires which were mounted in the direction of the laser beam with five millimeters spacing. These pins were of different lengths to simplify the identification of the region in the cell viewed by the camera. The center pin was the highest and placed approximately 2.5 mm below the center of the cell such that it still could be seen in the picture but was sufficiently away from the developing hydrogen plasma as not to interfere with the plasma cloud during the first 700 nanoseconds of development. The camera was triggered by the  $t_{out}$  triggering mechanism of the Korad K-1 power supply which occurred approximately 350 nanoseconds before the K-D1 photodiode triggered. The  $t_{out}$  signal was then electronically delayed by a Tektronix 7704 oscilloscope delay triggering circuit to allow for a consecutive series of time dependent plasma shots. The camera was operated in the framing mode with  $75 \times 10^6$  frames per second. In order to obtain the necessary details all shots were done in the five frames per picture mode such that each frame contained the information of 8 nsec exposure separated by 13.3 nsec from the next frame.



The alignment of the whole system was checked daily with the helium neon laser. The delay mirror system had to be checked frequently during the experimental runs in order to get a reference beam of optimal strength. The alignment of the pressure cell was less critical due to the rigid mounting table employed. It was therefore found to be sufficient to check the optical axis of the pressure cell every other day with the help of hole masks that could be fitted into the entrance and exit windows.

Intensities of both the cell and the reference beam were matched to the same signal height on the oscilloscope by neutral density filters and infrared absorption filters behind the pressure cell. These filters were carefully selected for a constant absorption percentage in the spectral region of interest. This matching of the signal strength of both beams allowed the observation of both signals on the Tektronix 7904 scope at the same time. Pictures from the scope were taken with a Polaroid camera providing instant read-outs.







#### IV. DATA

The data in this study were taken in two areas of interest: the spectral distribution of the forward scattered light and the time dependent development of the hydrogen plasma inside the cell. The spectral distribution of the forward scattered light was obtained by scanning the wavelength region between 10,300 and 10,900 Å. It was discovered that the laser used did not only transmit at the wavelength for neodymium glass lasers, 10,640 Å, but also at a second wavelength with a reduced intensity of  $1/200^{\text{th}}$  of the intensity at 10,640 Å. This wavelength was measured through the whole pressure range from 20 millitorrs to ten atmospheres as 10,470 Å. It is believed to be caused by impurities in the laser rod used. Reference 18 lists a wavelength of this order for a Nd- $\text{CaF}_2$  laser. Since the intensity of this line was so small compared to the central line it has not been plotted.

Since the neodymium laser was used in the pulsed mode, every laser shot had to be checked if it created the same conditions for plasma development. It was found that the observation of the time difference between the cell pulse and the reference pulse was a useful criterion to sort out "bad shots". These "bad shots" were believed to be caused by erratic absorption which might have been due to



anomalous absorption or a delay in the onset of breakdown. Since the pressure stayed the same it was not easy to see how the collisional absorption rate could change by a factor of up to seven. An explanation for this behavior has yet to be found.

In Figure 2b the time difference between the occurrence of the laser peak pulses at different pressures is plotted. The reference time ( $t=0$ ) for this diagram is the occurrence of the cell beam peak at a pressure of 20 millitorrs (see Fig. 2a). It was assumed that at this low pressure no absorption could take place inside the pressure cell. This was checked by a photodetector (see Ref. 11) and by the use of laser footprint burn pattern paper in front of and behind the pressure cell at 20 millitorrs pressure. Since the burn patterns exhibited the same intensity for the same energy in the laser pulse this assumption appears valid.

As seen in Figure 2b, with increasing pressure absorption set in at an earlier time with respect to the pulse maximum at 20 mTorr. At the moment of breakdown absorption reduces the transmitted laser light. Hence, the apparent peak of the transmitted pulse occurs shortly after breakdown. This peak is considerably smaller than the original pulse maximum. The time of occurrence of the peak in the transmitted light came earlier with increasing pressure, from -8 nsec at one atmosphere pressure to -20 nsec at three atmospheres. A further increase in pressure showed no additional time change and



thus the onset of absorption from three to ten atmospheres pressure was constant at  $\sim 20$  nanoseconds before the vacuum pulse maximum would have occurred. This time dependence of the onset of absorption was always checked by the occurrence of the maximum of the reference pulse which traveled through air around the cell. Since breakdown did not take place due to the smaller amount of energy contained in this pulse and the mirror losses during the reflections, the occurrence of this pulse was fixed as a reference timemark on the signal traces displayed by the oscilloscope. This timemark was also chosen to allow for a time jitter in the trigger circuit. Since both signals were traced on the scope using the same trigger signal these errors could be eliminated. The time difference between both, the reference and the cell beam, increased with pressure in the display on the oscilloscope from 87 for the vacuum shot to 107 nanoseconds at ten atmospheres. Figure 2b was constructed subtracting the time difference of 87 nsec for the vacuum shot from the time difference of the shots at higher pressures.

Another criterion was the ratio of the signal height of the cell beam to the reference beam. Although the signals of both pulses were set at an equal height at a fixed wavelength, it was found that some shots at the same pressure and wavelength setting produced large variations in this ratio. Since always at least three shots were taken at the same settings it was possible to sort out "bad





shots" with an abnormally large or small ratio. This ratio of the cell beam to the reference beam did not exhibit a wavelength or energy dependence. It could therefore only be used for the same pressure and wavelength setting. The fact that pulses of different ratios occurred could only be explained by the assumption of different conditions in the plasma formation. It was observed that laser shots did not always have the same halfwidth time because the laser profile obtained frequently during experimental runs exhibited halfwidth times between 20 and 30 nanoseconds. Since the onset of absorption depended on a certain laser power threshold and probably the presence of some electrons in the focal volume the breakdown may have occurred at different times during the laser pulse. Thus shots with quite different ratios between the cell beam and the reference beam had to be discounted because they did not represent the same plasma conditions due to either anomalous heating effects in the plasma or reflection of the light. The actual cause for these erratic shots has not yet been determined. It was believed, however, that these two criteria allowed a good judgement for the admission of subsequent shots that reproduced the same plasma conditions.

In order to get information about the wavelength dependence of absorption, a series of laser shots was made at three different wavelength settings,  $10,614 \text{ \AA}$ ,  $10,636 \text{ \AA}$ , and  $10,658 \text{ \AA}$ . These wavelength settings represented the central laser line at  $10,636 \text{ \AA}$  and





two wavelengths  $22 \overset{\circ}{\text{Å}}$  from the central laser line to both sides. The pressure was varied from 20 millitorrs to 8.1 atmospheres in steps of 1.02 atmospheres which is equivalent to 15 psi on the laboratory gauge used. The resulting data are displayed in Figure 3.

It can be seen that the fractional absorption is about the same for the two sidelines. The center line, however, exhibited a smaller fractional absorption in the regime of lower pressures up to three atmospheres. It is believed that the stronger intensity of the center laser line which has been measured to be approximately 20 times stronger than the sidelines caused this effect. Another explanation could be that the percentage of the forward scattered light peaks around the central laser line while for larger or smaller wavelengths the amount of the side-scattered light is increased. This can only be shown in a spectral analysis of the side-scattered light. It was therefore decided to look at this spectral distribution in a future study.

This frequency dependent absorption should cause a steeper slope in the spectral distribution of the cell beam when breakdown occurred in the pressure cell. The dependence of the onset of breakdown on pressure was shown in a previous study by Jim Carlisle [Ref. 11]. He found that breakdown occurred for the laser power densities used in this study if the pressure in the cell exceeded a value of 13.8 psia which is equivalent to 0.94 atmospheres. It can indeed be shown in Figures 5 to 8 that this is the case. The



reference beam which is plotted in these diagrams with an interrupted line exhibits a much broader pulse shape than the cell beam plotted above.

The spectral profiles in Figures 4 to 8 had to be normalized to allow a comparison of subsequent laser shots because the energy in each shot could not be held constant. The energy monitored by the K-D1 photodiode varied between 3 and 6 Joules per shot. It is proportional to the photon flux that reaches the UDT PIN 10 photodiode at the exit slit of the spectrograph. Thus a linear dependence of the signal strength from the PIN 10 diode to the energy output of the laser could be assumed. All pulses were thus normalized to the equivalent of a one Joule laser pulse.

The spectral profiles of the forward scattered laser light were obtained at different pressures ranging from 20 millitorrs to 9.16 atmospheres (134.7 psia). All profiles are given in arbitrary intensity units since it was necessary to use different filters to reduce the intensity of the forward scattered light in order to prevent damage to the spectrograph and the photodiode. The relation between the absolute intensity and the reduced intensity at the photodiode was determined by the transmission curves of the filters used and by direct measurement in the case of Figures 4 and 5 where slits have been used at a fixed wavelength outside the maximum intensity line. The wavelength was predialled depending on the wavelength region observed



at steps from  $34 \text{ \AA}^{\circ}$  at the tails decreasing to  $3.4 \text{ \AA}^{\circ}$  around the peak of the spectral distribution. Frequent checks at intermediate settings down to  $0.34 \text{ \AA}^{\circ}$  showed no additional information and thus confirmed the validity of this approach.

The spectral profiles of Figures 4 to 8 showed that the forward scattered light varied only in absolute intensity due to the pressure dependent absorption. A wavelength shift as has been suggested in a previous work where no spectral resolution of the forward scattered light was possible [Ref. 11] could not be found. This can be observed clearly from the coincidence of the maxima in the spectral distribution of both the reference and the cell beam in figures 5 to 8. Although spectral distributions of the forward scattered light were obtained for many more pressure settings in steps of 0.68 atmospheres it was decided to display only selected spectral distributions in Figures 4 to 8.

The suggested frequency shift that could not be found in this study can be explained by Figure 4. In this diagram the spectral distribution of a series of vacuum shots is contrasted to the spectral distribution of a series of vacuum shots viewed through a 1.06 micrometer filter with a halfwidth of  $35 \text{ \AA}^{\circ}$ . Since the center laser line has been determined in this study to be at  $10,636 \text{ \AA}^{\circ}$  which is the published value for a neodymium glass laser [Ref. 18] the maximum in the distribution viewed through the filter should be shifted to the left towards





a shorter wavelength with respect to the unfiltered distribution. This is indeed what is observed in Figure 4.

The high speed image converter camera Imacon 600 was used in the frame mode with five frames per laser shot. The time separation of the frames was 13.33 nsec, calculated from the framing unit constant of  $7.5 \times 10^7$  frames per second. Thus it was possible to measure the generation and dynamics of the plasma during the laser pulse. Due to the delay circuit of the oscilloscope the time of arrival at the center of the pressure cell could be determined with nanosecond accuracy. Band pass filters, long pass filters, and neutral density filters had to be used in order to reduce the intensity of the side-scattered light. The initial stage of the plasma development during the laser pulse is shown in Figure 9a. With the laser impinging from the right, isolated plasma blobs are formed from the moment the laser light reaches the focal volume. These plasma blobs could only be observed when the laser light was on. Therefore it is believed that what is observed is laser light scattered at an angle of 90 degrees by the plasma blobs. However, when viewed through the narrow band 1.06 micrometer filter (Figure 4), no light could be observed. On the other hand, with a high pass filter with cutoff at  $7,800 \text{ \AA}$  the scattered light could again be observed. Therefore it appears the wavelength of the observed scattered light has to be longer than  $7,800 \text{ \AA}$  but not precisely  $10,600 \text{ \AA}$ . The exact wavelength of this light has not been measured





due to a lack of appropriate narrow band pass filters. It was observed that the plasma blobs viewed through the high pass filter were only visible as long as the laser light was on. They were visible, however, after laser shutoff in other wavelength regions.

For a pressure above three atmospheres absorption sets in 20 nanoseconds before the laser pulse reaches its peak (Figure 2a). Thus it should be expected to have absorption taking place over a time span of 40 nsec. This has indeed been observed (Figure 9b). The side-scattered light coincided with the duration of the laser pulse and ceased after 40 nsec. The velocity of the breakdown region in the upstream motion toward the laser beam was found to range from  $1.25 \times 10^4$  m/sec to  $1.5 \times 10^5$  m/sec. This is in agreement with data published in the current literature [Ref. 14]. The diameter of the blobs was measured to be from 0.05 to 0.1 mm. Compared to the focal spot diameter of 0.09 mm this may be taken as evidence for the occurrence of self-focusing effects in the plasma. A plasma blob created 4 mm in front of the focal spot should have a radial extension of 1.4 mm after a path of the breakdown region of 4 mm in 40 nsec at a velocity of  $10^5$  m/sec. Actually the size is considerably smaller, namely 0.05 mm from Figure 9b. Thus it is believed that self-focusing effects in the plasma confined the blobs to a size an order of magnitude smaller than expected.

Some photos seem to indicate two filaments in front (Figure 10b). From Figure 10a it is seen that the propagation of the plasma is faster



in the longitudinal direction than in the radial direction. Speeds of  $4.17 \times 10^4$  m/sec and  $1.25 \times 10^4$  m/sec are measured in the longitudinal and radial direction respectively. This gives rise to the characteristic shape of the developing plasma in Figure 11a.

With the help of the delay circuitry the plasma light could be photographed over a wide time range. For about 800 nsec the plasma emitted light was observable and became more and more diffuse in shape as time went on. In order to gain more insight into the structure of the expanding plasma different filters had to be used. The prominent emission line of hydrogen is the  $H_\alpha$  line. A filter for this wavelength revealed that the main light from the plasma is indeed in this wavelength region (Figure 11b). This showed furthermore that the plasma light is more evenly distributed along the laser axis in comparison with Figure 11a where without filters all visible wavelengths of the emitted light are present. Thus high speed photography provided a powerful tool for the analysis of the plasma properties.



## V. RECOMMENDATION

During the study it became obvious that many laser shots had to be taken at the same wavelength and pressure settings because not all of the shots reproduced the same plasma conditions. Although the criteria of the onset time of absorption and the ratio between the cell beam and reference beam intensities proved to be useful to sort out "bad shots", it was strongly felt that a recording means for the whole spectral distribution of a single laser shot was desirable. Since the photographic technique is hampered around the neodymium laser line by the cutoff wavelength of about 950 nm for commercially available photographic emulsions, it is recommended to obtain the spectral profile by using a laser in the visible regime. Such a laser is available in the same high power configuration with a pulsed ruby laser.

It is further recommended to study the spectral distribution of the side-scattered light with a reconstructed pressure cell especially for this purpose. This cell should allow the measurement at different angles from the laser beam axis in order to get a better insight into the dynamics of the expanding plasma.

It is also of great value to observe the self-focusing effect with focusing lenses of shorter focal length, for Alcock [Ref. 14] has observed less plasma blobs with a 2.5 cm focal length lens. The



structure of the plasma blobs could be made more clear by using optical systems on the camera that enhance the magnification.

It is finally suggested to use magnetic probes in order to investigate the self-generated magnetic field of the plasma. The reproducibility of the plasma generation could be improved by preionizing the gas. This seeding of the gas with electrons may also provide a better onset of breakdown and help to avoid "bad shots".





# Experimental Setup

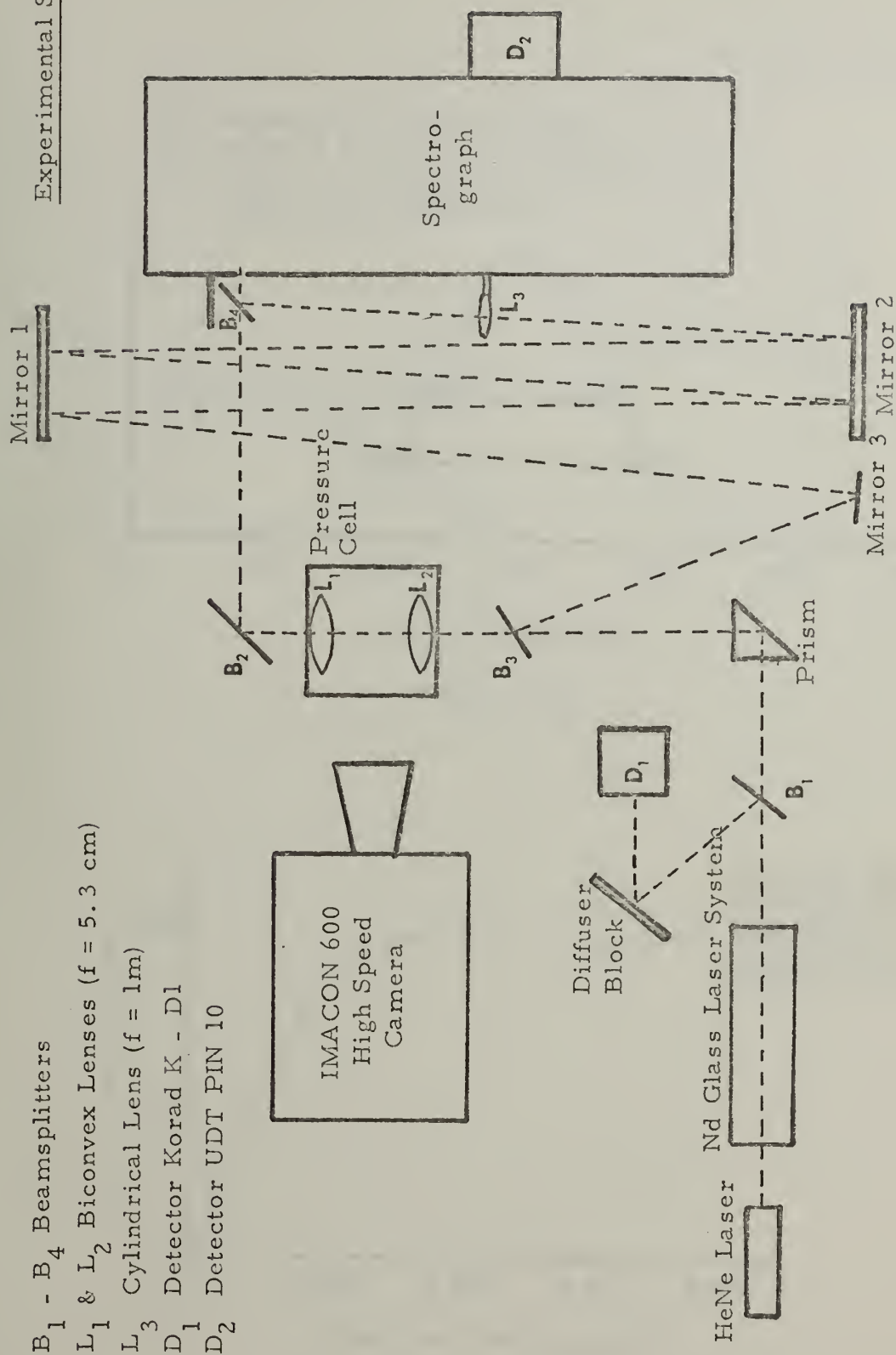


Figure 1



## Laser Profile

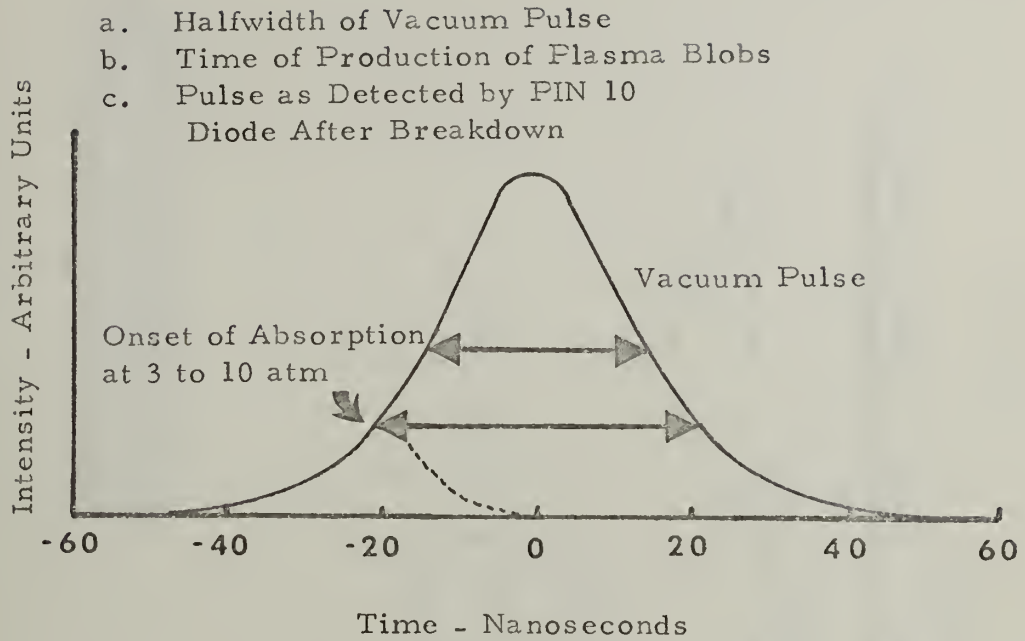


Figure 2a

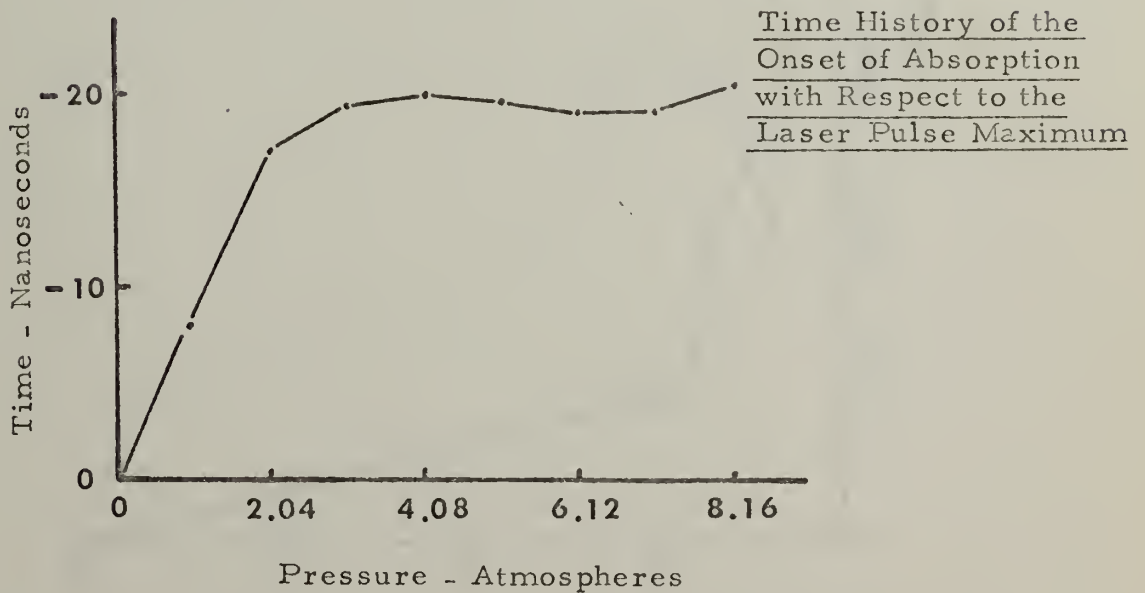


Figure 2b



Relative Intensity of the Forward  
Transmitted Light Versus Pressure  
for Three Selected Wavelengths

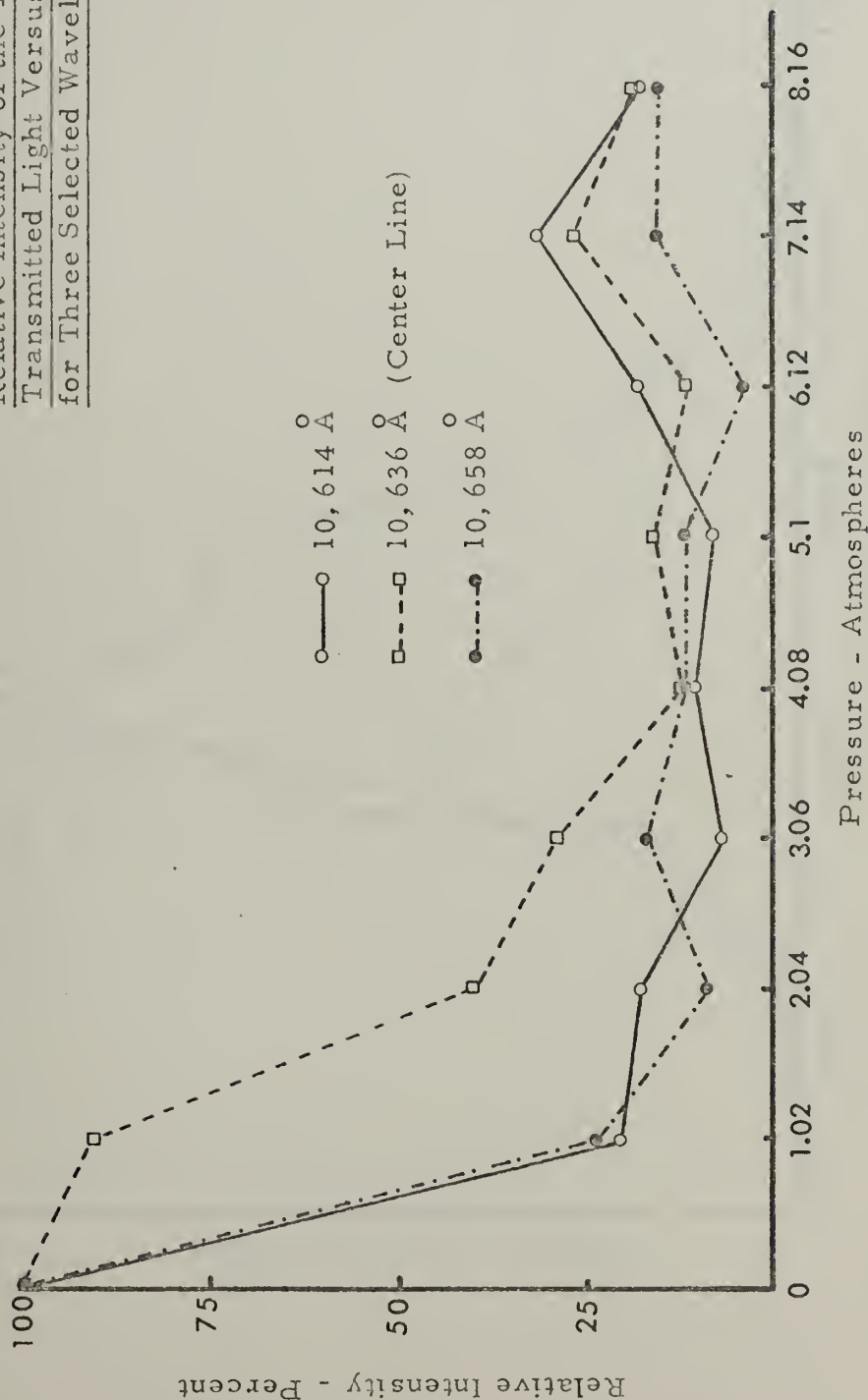
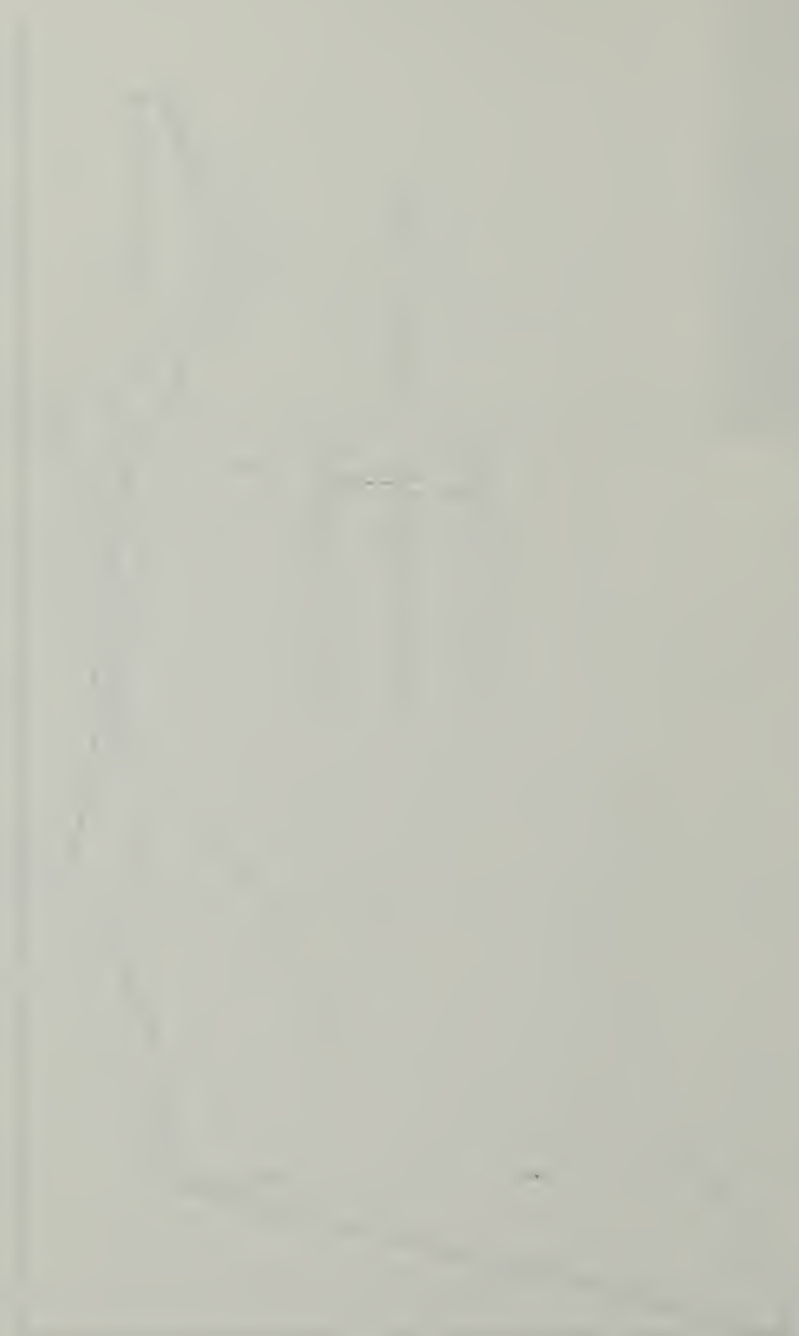


Figure 3



Spectral Distribution at a  
Pressure of 20 Millitorr

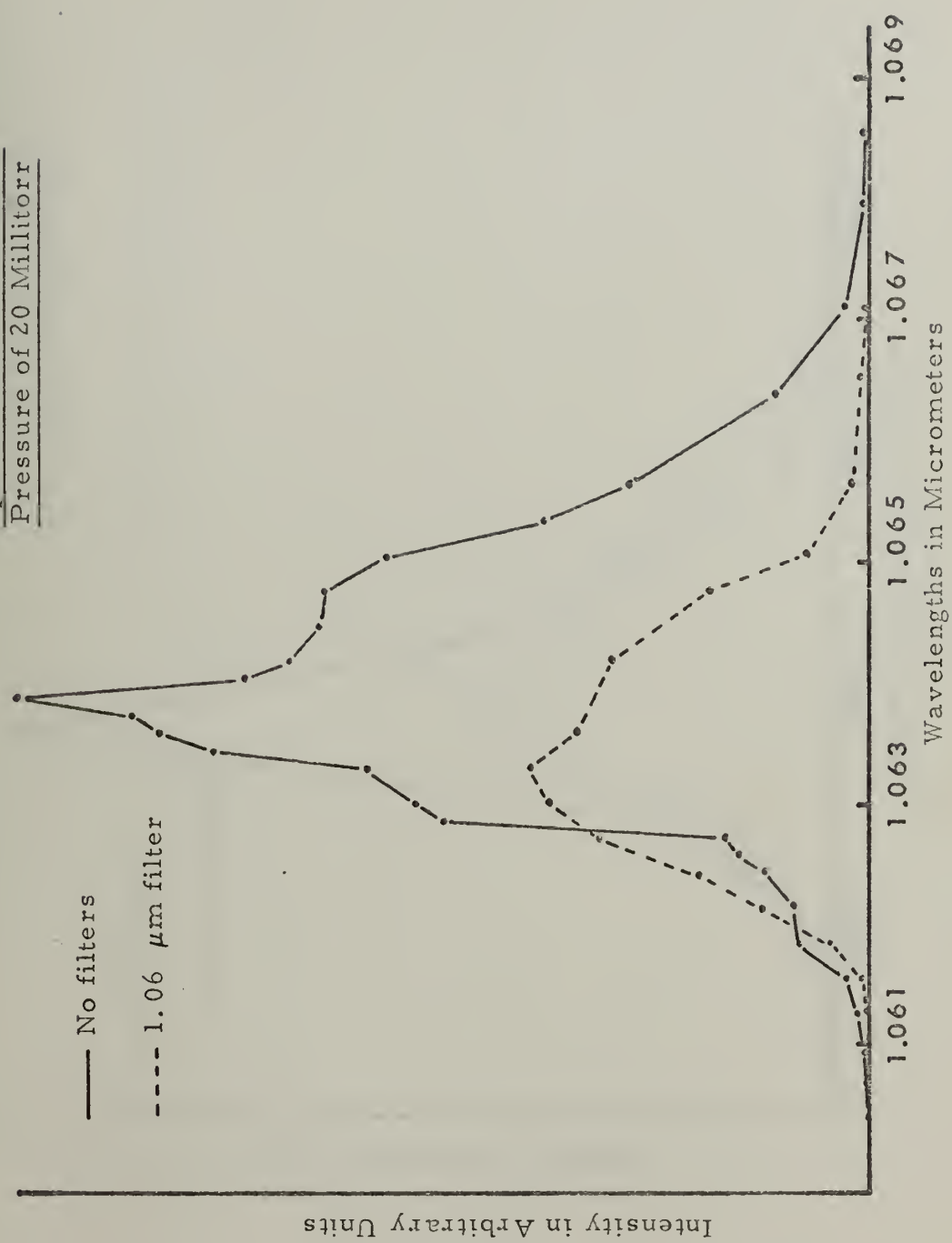


Figure 4





Spectral Distribution at a  
Pressure of 1 Atmosphere  
 (14.7 psia or 0 psi gauge)

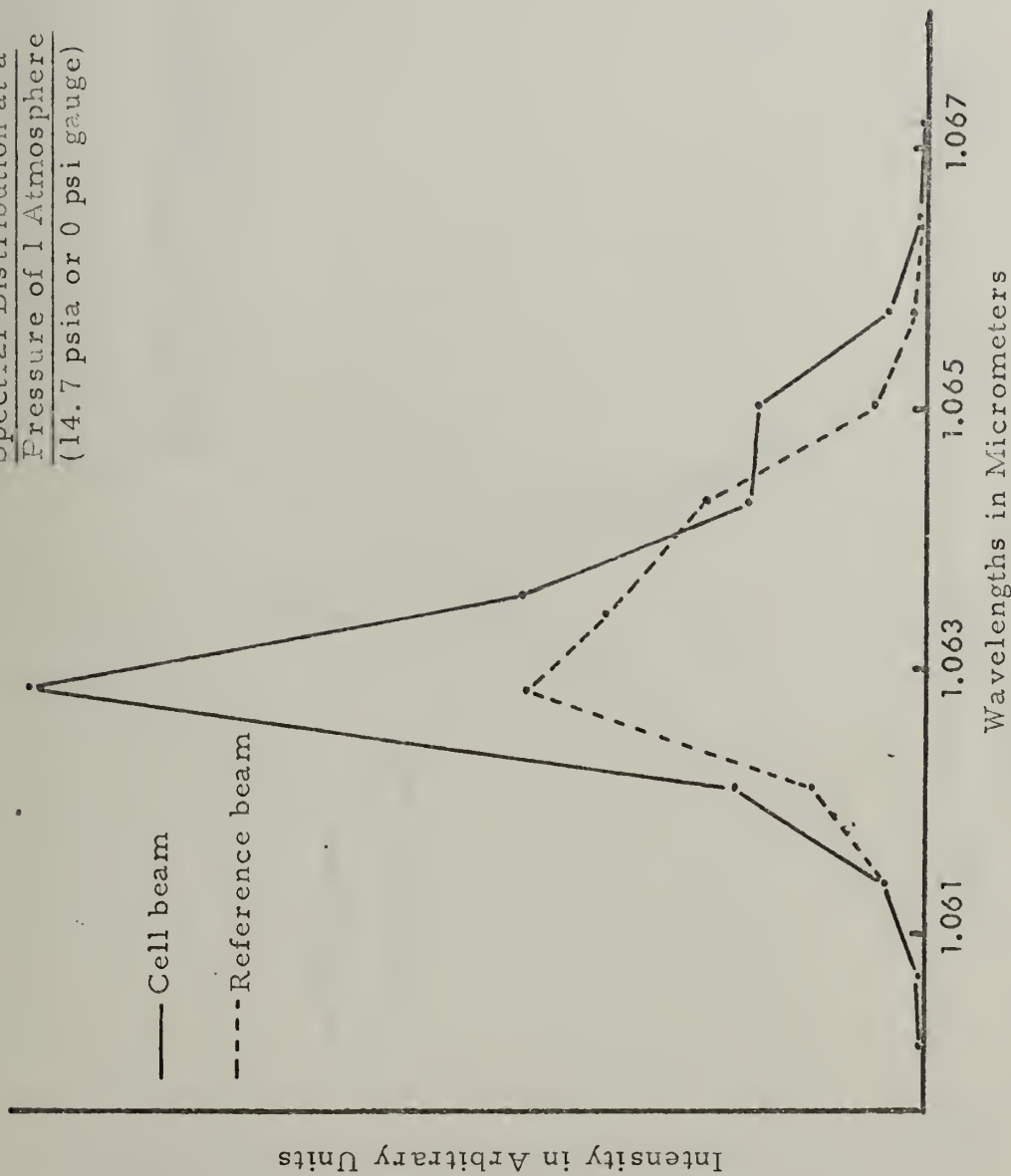


Figure 5



Spectral Distribution at a  
Pressure of 2.36 Atmospheres  
 (34.7 psia, 20 psi gauge)

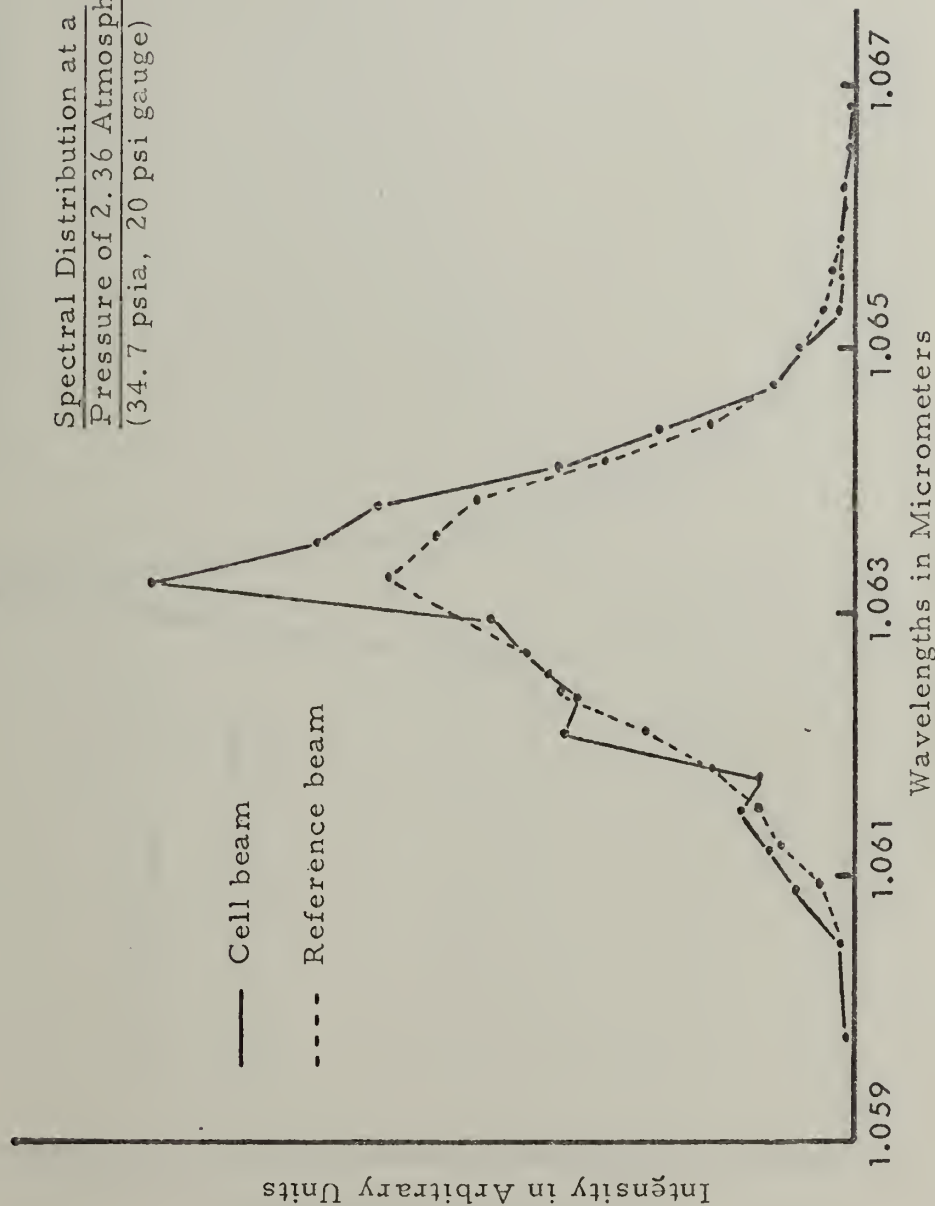


Figure 6



Spectral Distribution at a  
Pressure of 3.72 Atmospheres  
(54.7 psia, 40 psi gauge)

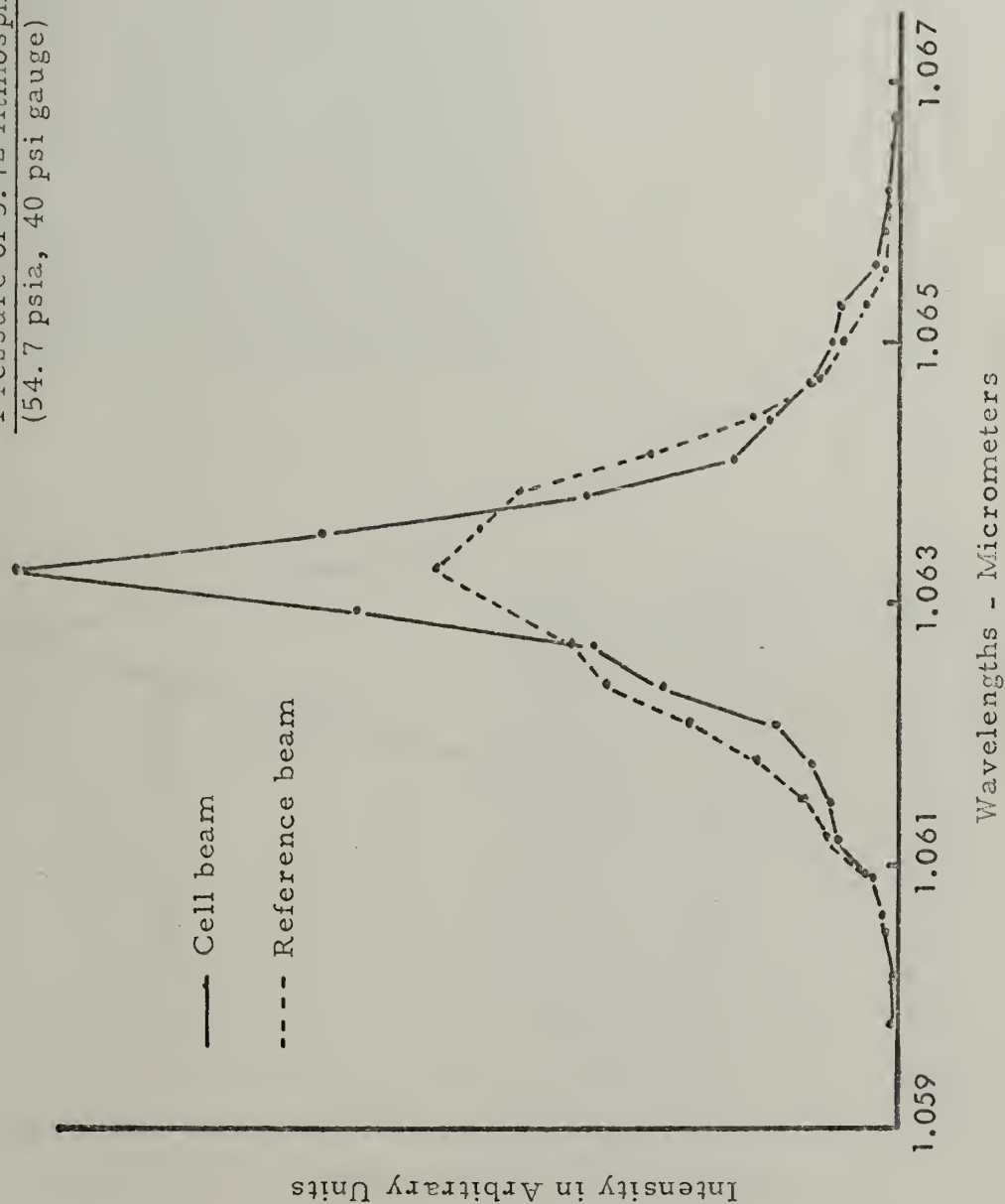


Figure 7





Spectral Distribution at a  
Pressure of 9.16 Atmospheres  
 (134.7 psia or 120 psi gauge  
 pressure)

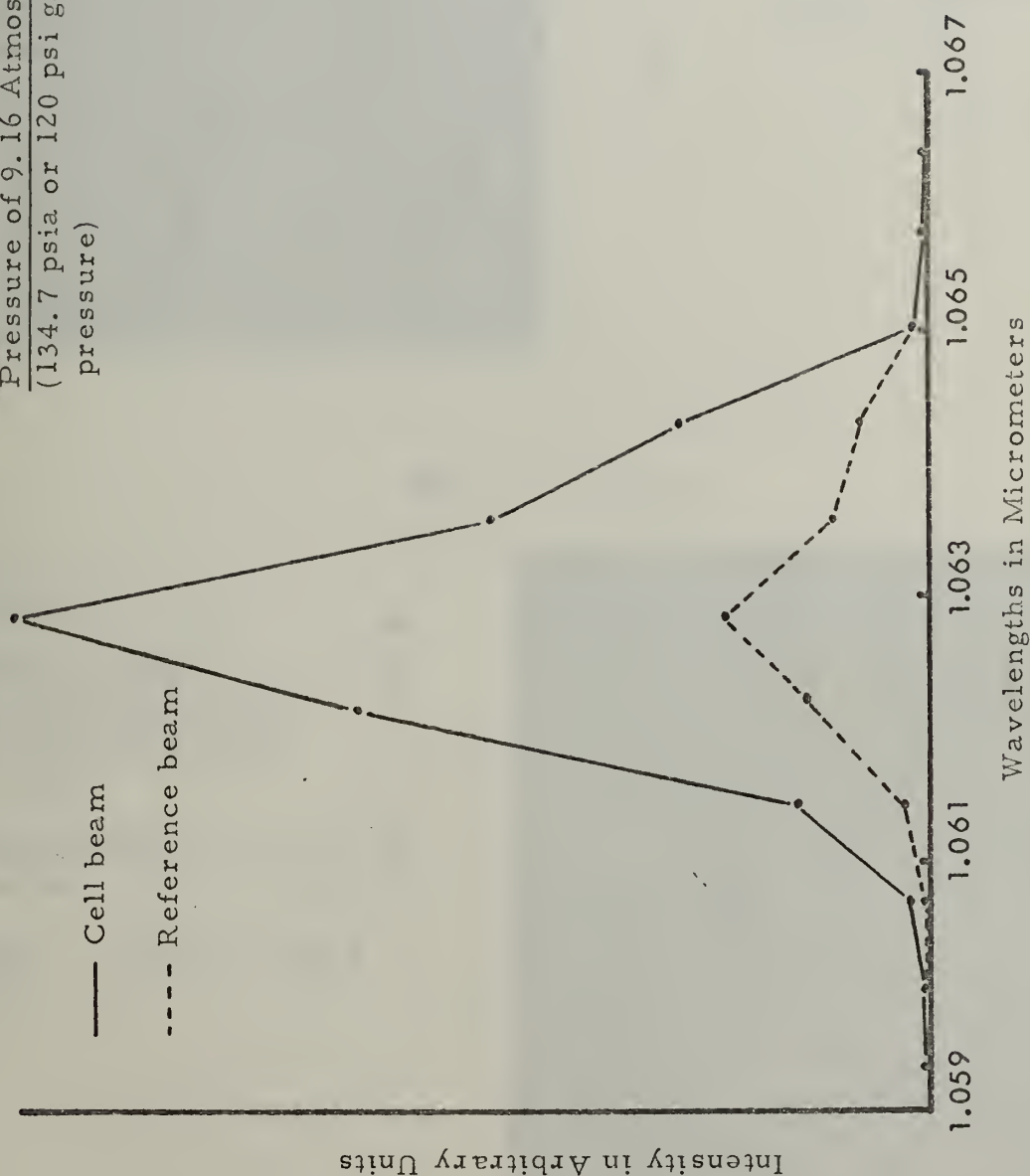


Figure 8





Figure 9a

Self-Focusing in  
Hydrogen Plasma  
for the First 20nsec  
at 3 atm

Magnification 6 times

Filter: Highpass 7800 Å  
Iris : 11

↑  
TIME

← LASER

Figure 9b

Self-Focusing  
in Hydrogen Plasma  
for the Last 20 nsec  
at 3 atm

Magnification  
8 times

Filter: Highpass 7800 Å  
Iris : 4

↑  
TIME

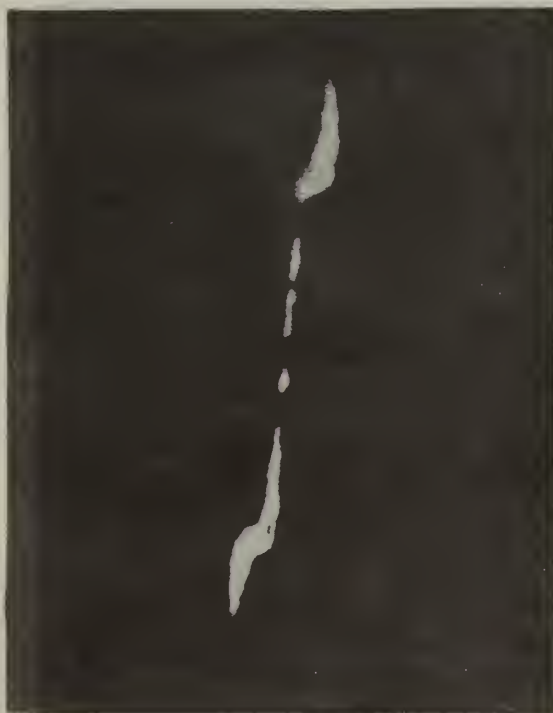






Figure 10a

Self-Focusing in  
Hydrogen Plasma  
at 3 atm

(Last 20 nsec  
observed with no  
filters)

Magnification 9 times

Filter: Bandpass 4400 Å<sup>o</sup>  
Infrared Absorption  
10% Neutral Density

Iris: 11

↑  
TIME

← LASER

Figure 10 b

Plasma Structure  
After 100 nsec

Magnification  
2 times

Filter: Bandpass 4400 Å<sup>o</sup>  
Infrared Absorption  
10% Neutral Density

Iris: 8

↑  
TIME







LASER  
 ↓  
 ↑  
 TIME

Figure 11a

Structure of the  
Hydrogen Plasma  
at 3 atmospheres

(Without filters at  
arrival of the laser  
pulse)

Magnification 8 times

Filter: None

Iris : 11

← LASER

Figure 11b

Structure of the  
Hydrogen Plasma  
Viewed through  
 $H_{\alpha}$  - Filter 100 nsec  
After Arrival of  
Laser Pulse

Magnification  
2 times

Filter : H

Iris : 4

↑  
 TIME







## LIST OF REFERENCES

1. Decroisette, M. et al., "Induced Compton Scattering and Non-linear Propagation in Laser-Created Plasmas," Physical Review A, vol. 5 no. 3, p. 1391-1396, March 1972.
2. Ready, J. F., Effects of High-Power Laser Radiation, p. 213-271, Academic Press, 1971.
3. Hudson, R. D., Infrared Systems Engineering, p. 180, Wiley-Interscience, 1969.
4. Max-Planck-Institut für Plasmaphysik Report IPP, Observation of High-Order Raman Antistokes Radiation and Its Role in the Initial Phase of Plasma Production by Lasers, by H. Mennicke, p. 5, 12. July 1972.
5. Ahmad, N. et al., "Plasma Temperature in a Laser Produced Gas Breakdown," J. Phys. B: Atom.Molec.Phys., vol. 5, p. 875, April 1972.
6. de Montgolfier, P., "Laser-Induced Gas Breakdown: Electron Cascade," J.Phys. D: Appl.Phys., vol. 5, p. 1443, April 1972.
7. Soloukhin, R. I. et al., "Hydrogen Plasma Absorption Coefficients at Laser Frequencies," J.Quant.Spectrosc.Radiat.Transfer, vol. 12, pp. 25-34, February 1972.
8. Dawson, J., "On the Production of Plasma by Giant Pulse Lasers," The Physics of Fluids, vol. 7, p. 981-987, July 1964.
9. Princeton University Report MATT-817, Anomalous Heating of Plasmas by Laser Irradiation, by P. Kaw et al., p. 5, 17. December 1970.
10. Editors, "Berichte: 1969 Annual Meeting of the Division of Plasma Physics," LASER und angewandte Strahlentechnik, Nr. 1/1970.
11. Carlisle, J. A., Laser Light Absorption Characteristics of a Laser Produced Hydrogen Plasma, M. S. Thesis, Naval Postgraduate School, Monterey, 1972.



12. United Kingdom Atomic Energy Authority Report CLM-R 109, Lasers and the Reactor Ignition Problem, by I. J. Spalding, p. 3, 15. November 1970.
13. Dubois, D. F. et al., "Parametrically Excited Plasma Fluctuations," Physical Review, vol. 164, p. 207, December 1967.
14. Alcock, A. J., "Experiments on Self-Focusing in Laser-Produced Plasmas," Laser Interaction and Related Plasma Phenomena, vol. II, Plenum Press, 1972.
15. Kerr, E. L., "Filamentary Tracks Formed in Transparent Optical Glass by Laser Beam Self-Focusing. II. Theoretical Analysis," Physical Review A, vol. 4 no. 3, September 1971.
16. Hora, H., Self-Focusing and Nonlinear Acceleration Process in Laser Produced Plasmas, " Opto-Electronics, Nr. 2, 1970.
17. Naval Research Laboratory Report 7301, Demonstration of Collisionless Interactions Between Counterstreaming Ions in a Laser-Produced Plasma Experiment, by S. O. Dean, p. 9, 17 September 1971.
18. Radio Corporation of America, Electro-Optics Handbook, p. 9-3, 1968.



### INITIAL DISTRIBUTION LIST

	No. Copies
1. Defense Documentation Center Cameron Station Alexandria, Virginia 22314	2
2. DOKZENT Bundeswehr-See 53 Bonn Friedrich - Ebert - Allee 34 Fed. Rep. of Germany	2
3. Marineamt In EBM 294 Wilhelmshaven Fed. Rep. of Germany	2
4. Library, Code 0212 Naval Postgraduate School Monterey, California 93940	2
5. Assoc. Professor Fred R. Schwirzke Code 61Sw Department of Physics Naval Postgraduate School Monterey, California 93940	3
6. Kurt D. Wachsmuth, LCDR FGN 7 Moreland Ave., #25 Pacific Grove, California 93950	1
7. Inst. Nat Ceglio Code 61 Department of Physics Naval Postgraduate School Monterey, California 93940	1





Unclassified

Security Classification

## DOCUMENT CONTROL DATA - R &amp; D

(Security classification of title, body of abstract and indexing annotation must be entered when the overall report is classified)

1. ORIGINATING ACTIVITY (Corporate author)		2a. REPORT SECURITY CLASSIFICATION	
Naval Postgraduate School Monterey, California 93940		2b. G#DUP	
3. REPORT TITLE			
Spectrometric and Photographic Analysis of a Laser-Produced Hydrogen Plasma			
4. DESCRIPTIVE NOTES (Type of report and inclusive dates)			
Master's Thesis; June 1973			
5. AUTHOR(S) (First name, middle initial, last name)			
Kurt D. Wachsmuth			
6. REPORT DATE		7a. TOTAL NO. OF PAGES	7b. NO. OF REFS
June 1973		50	18
8a. CONTRACT OR GRANT NO.		9a. ORIGINATOR'S REPORT NUMBER(S)	
b. PROJECT NO.			
c.		9b. OTHER REPORT NO(S) (Any other numbers that may be assigned this report)	
d.			
10. DISTRIBUTION STATEMENT			
Approved for public release; distribution unlimited.			
11. SUPPLEMENTARY NOTES		12. SPONSORING MILITARY ACTIVITY	
		Naval Postgraduate School Monterey, California 93940	

## 13. ABSTRACT

Light from a neodymium glass laser was focused in hydrogen gas at pressures from 20 mTorr to 9.16 atm in order to produce optical breakdown. The forward scattered light from the breakdown region was spectrally analyzed with a grating spectrograph from 10,300 to 10,900 Å. It was found that the spectral distributions exhibited no distinguishable frequency shift. However, the absorption of the laser light depended on frequency and gas pressure. The time dependence of the onset of absorption was determined by comparing the cell beam with a beam-split reference beam that bypassed the pressure cell. The light scattered at an angle of 90° was photographed with a high speed image converter camera in the framing mode. This revealed evidence of self-focusing during the time the laser light was on. The plasma parameters were calculated from the kinetic theory of ideal gases and the theory of ionized gases, assuming complete ionization. The results of this study were compared to results published in the current literature. Agreement was good, especially in the case of self-focusing.



KEY WORDS	LINK A		LINK B		LINK C	
	ROLE	WT	ROLE	WT	ROLE	WT
Plasma, Hydrogen, Laser spectral Distribution High-Speed Photography						













Thesis  
W12  
c.1

Wachsmuth

144077

Spectrometric and  
photographic analysis  
of a laser-produced  
hydrogen plasma.

Thesis

144077

W12  
c.1

Wachsmuth

Spectrometric and  
photographic analysis  
of a laser-produced  
hydrogen plasma.

thesW12

Spectrometric and photographic analysis



3 2768 001 92829 4

DUDLEY KNOX LIBRARY